ACS Catalysis

Research Article

pubs.acs.org/acscatalysis

# Low-Temperature $CO_2$ Hydrogenation to Liquid Products via a Heterogeneous Cascade Catalytic System

Yuan Chen, Saemin Choi, and Levi T. Thompson*

Department of Chemical Engineering and Hydrogen Energy Technology Laboratory, University of Michigan, Ann Arbor, Michigan 48109-2136, United States

**ABSTRACT:** Research described in this paper targeted a cascade system for the hydrogenation of $CO_2$ to methanol via formic acid and/or formate intermediates, a reaction sequence that has been accomplished previously using homogeneous catalysts. On the basis of results for the hydrogenation of $CO_2$, formic acid, and ethyl formate over a series of Cu- and $Mo_2C$-based catalysts, we selected a Cu chromite catalyst for $CO_2$ hydrogenation to the formate and a Cu/$Mo_2C$ catalyst to convert the formate to methanol. These catalysts worked cooperatively in the presence of ethanol, yielding a methanol turnover frequency of $4.7 \times 10^{-4}$ $s^{-1}$ at 135 °C, 10 bar of $CO_2$, and 30 bar of $H_2$ in 1,4-dioxane. The performance for this Cu chromite:Cu/$Mo_2C$ cascade system surpassed the additive production of the individual catalysts by ~60%. The results also allowed an investigation of the reaction pathways. The hydrogenation of $CO_2$ to formic acid appeared to be the rate-limiting step for most of the catalysts. This is not surprising given the thermodynamics for this reaction. Finally, the hydrogenation of $CO_2$ to dimethyl ether was also demonstrated using a system consisting of the Cu/$Mo_2C$ catalyst to produce methanol from $CO_2$ and HZSM-5 to produce dimethyl ether from methanol. The systems described in this paper are, to our knowledge, the first demonstrating cascade $CO_2$ hydrogenation via heterogeneous catalysts.

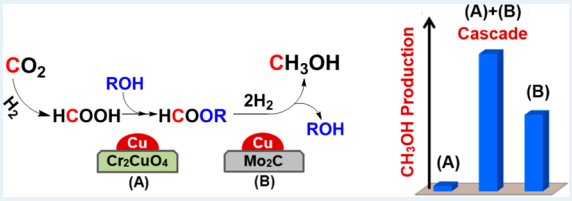


**KEYWORDS:** *$CO_2$ hydrogenation, low temperature, methanol synthesis, cascade catalysis, heterogeneous catalysis, $Mo_2C$-based catalysts, Cu-based catalysts, reaction pathways*

## INTRODUCTION

The production of chemicals and fuels consumes more than 4 Gton of carbon per year, most of which comes from fossil resources.[1] With growing evidence linking anthropogenic $CO_2$ emissions to global climate change, there has been an increased interest in finding nonfossil carbon sources.[2] Advances in carbon capture could facilitate the use of $CO_2$ as a source of carbon. $CO_2$ is abundant and its hydrogenation, using hydrogen from renewable sources (e.g., $H_2O$), could result in a sustainable route for the production of chemicals and fuels.[3] Of course, processes are being developed to convert biomass into chemicals and fuels; however, their impact could be limited by the slow biological rates for biomass production from $CO_2$, significant land use requirements, and other environmental challenges.[4] Nonbiological processes convert nearly 100 Mton of $CO_2$ into products including urea and polycarbonate plastics; nevertheless, the large-scale production of commodity chemicals or fuels from $CO_2$ has been limited due to the lack of sufficiently active and selective catalysts.[3a] A desirable first product from $CO_2$ is methanol, an essential precursor to a variety of useful products such as olefins (via the methanol to olefins process[3b]), gasoline (via the methanol to gasoline process[5]), biodiesel,[6] and a fuel or fuel additive. The hydrogenation of $CO_2$ to methanol not only recycles $CO_2$ but also stores the chemical energy from $H_2$ with greater portability and potential to utilize established infrastructures.[7]

Conventional processes for $CO_2$ hydrogenation involve gas phase catalytic conversion over Cu−Zn based catalysts at high operating temperatures (230−270 °C), where methanol production is unfavorable due to the exothermicity of the reaction ($\Delta H_{298\ K}$ = −49.5 kJ/mol).[8] There have been significant efforts to improve catalyst performance; however, progress has been limited.[8b−d,9] Furthermore, $CO_2$ reduction to methanol is a multiple electron ($6e^-$) transformation, and the use of a single catalyst to achieve good performance could be challenging.[10]

Lower temperature thermochemical and electro-/photoelectrochemical methods have also been investigated for the conversion of $CO_2$ to methanol. Fan et al. employed Cu-based catalysts to hydrogenate $CO_2$ to methanol through formic acid and ethyl formate intermediates in liquid ethanol at 150−220 °C.[11] The Cu−Zn-based catalyst was most active and, at temperatures near 200 °C, yielded the maximum methanol selectivities. Yu et al. recently reported the use of a Cu−Zn−Al catalyst for the production of methyl formate from $CO_2$ in liquid methanol at 150−190 °C.[12] They proposed that the pathway involved the reaction of a surface formate with methanol to produce methyl formate; however, the conversion of methyl formate to methanol was not reported as the

Received: October 27, 2014
Revised: December 24, 2014
Published: February 2, 2015





DOI: 10.1021/cs501656x
ACS Catal. 2015, 5, 1717−1725

methanol being produced could not be distinguished from the methanol reaction media. A number of electro-/photoelectrochemical materials, including Cu- and carbon nanotube-based catalysts, have been developed for $CO_2$ hydrogenation.[13] Achieving high selectivities to methanol and high Faradaic efficiencies has proven to be a challenge as reduction potentials for methanol, formic acid, formaldehyde, and $H_2$ are similar.[14] Semiconductor materials, such as p-type gallium arsenide and p-type indium phosphide, have shown promising selectivities to methanol, however, at the expense of high overpotentials.[15]

Recently a cascade system involving homogeneous catalysts was demonstrated for the thermocatalytic conversion of $CO_2$ to methanol at low temperatures.[10,16] Cascade catalytic systems typically involve the use of multiple catalysts for sequential transformations within one pot or a single synthetic operation.[17] The individual catalysts are selected for specific reactions, and the increased degrees of freedom (i.e., using multiple catalysts) enhance the opportunities to optimize overall performance.[17,18] Huff and Sanford reported the use of a series of homogeneous catalysts for the cascade conversion of $CO_2$ to methanol at 135 °C through formic acid and formate ester intermediates (Figure 1).[10] Methanol turnover numbers

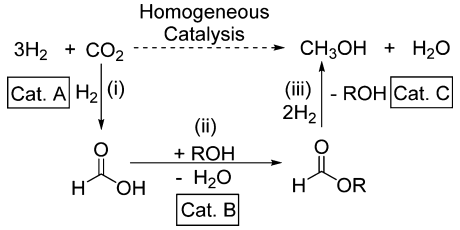


**Figure 1.** Cascade reaction pathway for $CO_2$ hydrogenation to $CH_3OH$ via formic acid and formate ester intermediates. Adapted from ref 10.

as high as 2.5 were reported for a one-pot 16 h reaction. A challenge for this system was incompatibility among some of the homogeneous catalysts as well as with the $CO_2$ reactant. Whereas the mechanisms that contribute to the incompatibility are being investigated,[19] suitable catalysts have not been reported. Heterogeneous catalysts could achieve greater compatibility and easier separation from the reactant/product mixture;[20] however, the use of heterogeneous catalysts for this type of cascade reaction has not been reported.

The primary objective of research described in this paper was to explore the feasibility of a low-temperature cascade system for the hydrogenation of $CO_2$ to methanol based on heterogeneous catalysts. Inspired by results reported by Fan et al.[11] and Huff and Sanford,[10] we targeted a system involving $CO_2$ hydrogenation through formic acid and/or formate ester intermediates. To design this system, we evaluated rates and selectivities for the hydrogenation of $CO_2$, formic acid, and ethyl formate over several Cu- and $Mo_2C$-based heterogeneous catalysts. Copper-based catalysts have been reported to be active for $CO_2$ hydrogenation to methanol[8b,9b] and are widely used for methanol synthesis from syngas, a mixture of CO and $H_2$ that often contains small amounts of $CO_2$.[21] Dubois et al.[22] and Xu et al.[23] reported that Mo carbides are active for the gas phase hydrogenation of $CO_2$ at 200−300 °C, producing mostly $CH_4$ and CO (~70%) and smaller amounts of methanol (~20%) and other hydrocarbons (up to $C_3$). Molybdenum carbide-based catalysts are also active for CO hydrogenation,[24] water−gas shift,[25] and hydrodeoxygenation[26] reactions. On the basis of the measured activities and selectivities over the Cu- and $Mo_2C$-based catalysts, we devised a cascade system and evaluated its performance for the hydrogenation of $CO_2$ to methanol. To the best of our knowledge, this is the first demonstration of an all-heterogeneous cascade system for this reaction. The results also enabled a prediction of the reaction pathways and key intermediates during $CO_2$ hydrogenation over the Cu- and $Mo_2C$-based heterogeneous catalysts.

## MATERIALS AND METHODS

**Catalyst Preparation.** Several commercially available Cu-based catalysts were acquired and used after pretreatment that is described later. These catalysts included $Cu/ZnO/Al_2O_3$ (Süd-Chemie/Clariant), $Cu/Cr_2CuO_4$ (Cu Chromite, Strem Chemicals Inc.), and nano-Cu (QuantumSphere). The $Cu/ZnO/Al_2O_3$ and $Cu/Cr_2CuO_4$ catalysts will be referred to as the Cu−Zn−Al and Cu−Cr catalysts throughout this paper. The nano-Cu catalyst was included to explore the importance of a support material. The high surface area $Mo_2C$ was synthesized using a temperature-programmed reaction (TPR) technique. Prior to the synthesis, ~1.3 g of ammonium molybdate (AM) precursor, $(NH_4)_6MO_7O_{24}{\cdot}4H_2O$ (Alfa Aesar), was sieved to 125−250 $\mu$m and then loaded into a quartz tube reactor. The AM was first reduced in $H_2$ flowing at 400 mL/min, as the temperature was increased from 25 to 350 °C in 70 min. Subsequently, the material was held at 350 °C for 12 h. The reaction gas was then switched to 15% $CH_4/H_2$ flowing at 400 mL/min; the temperature was increased to 590 °C in 1.5 h and maintained at 590 °C for 2 h before quenching to room temperature. The $Cu/Mo_2C$ catalyst was prepared using a wet impregnation method; the protocol for synthesizing this and other carbide-supported metals has been described in detail elsewhere.[27] Briefly, the freshly synthesized $Mo_2C$ was transferred under 15% $CH_4/H_2$ gas into a beaker containing 70 mL of deaerated water (to avoid the oxidation of $Mo_2C$) with 4.4 mg/L of $Cu(NO_3)_2$ and allowed to interact for 20 h. This method enabled the metal precursor to directly interact with the native $Mo_2C$ surface (as opposed to a passivated material). The resulting catalyst slurry was dried and reduced in situ in the reactor to decompose the nitrate and produce dispersed Cu domains.

**Catalyst Characterization.** Surface areas of the materials were measured using a Micromeritics ASAP 2010 analyzer based on $N_2$ physisorption. All of the catalysts were degassed (<5 mmHg) at elevated temperatures (Cu-based catalysts at 200 °C and $Mo_2C$-based catalysts at 350 °C) for 4 h prior to the surface area measurements. The bulk crystalline structures were characterized using X-ray diffraction (Rigaku Miniflex 600, Cu K$\alpha$ radiation) with 2$\theta$ ranging from 10° to 90° and a scan rate of 5°/min. Crystallite sizes were estimated via line broadening analysis using the Scherrer equation.[28] Metal compositions for the $Cu/Mo_2C$ catalyst were determined by inductively coupled plasma (ICP-OES) using a Varian 710-ES analyzer. Solutions for the ICP measurements were prepared by dissolving 15 mg of catalyst in 1.5 mL of aqua regia, consisting of 1.125 mL of HCl (Fisher Scientific) and 0.375 mL of $HNO_3$ (70%, Fisher Scientific). The solution was sonicated for 10 min and left for 10 h to allow complete dissolution. The resulting solution was diluted by a factor of 14 using ultrapure water (18 MΩ·cm, Millipore Hilli-Q Advantage A10) to achieve concentrations appropriate for the ICP analysis.


DOI: 10.1021/cs501656x
ACS Catal. 2015, 5, 1717−1725

The surface site densities for $Mo_2C$-based catalysts were determined via CO chemisorption. Prior to the measurements, the $Mo_2C$ and $Cu/Mo_2C$ catalysts were pretreated in 15% $CH_4/H_2$ for 4 h at 590 °C and then degassed in He at 600 °C for 1 h. The catalysts were cooled to 25 °C and repeatedly dosed with 5% CO/He (5 mL loop) until reaching saturation. To quantify the surface site densities for the other Cu-containing catalysts, a $N_2O$ decomposition technique was used. The Cu−Zn−Al and Cu−Cr catalysts were reduced in 10% $H_2$/Ar at 200 °C for 4 h and then degassed in He for 1 h. The catalysts were then cooled to 60 °C and exposed to a flowing mixture of 10% $N_2O$/He for 2 h. Followed by the $N_2O$ treatment, the sample was purged with He and cooled to 25 °C. A $H_2$ temperature-programmed reduction (TPR) was then performed by increasing the temperature from 25 to 400 °C in 10% $H_2$/Ar at 5 °C/min. The surface site density was determined by quantifying the $H_2$ consumed during TPR.[29] It should be mentioned that these chemisorbates ($N_2O$ and CO) cannot be used to independently determine the sites for Cu and $Mo_2C$ over the $Cu/Mo_2C$ surface, because $N_2O$ and CO adsorb to both Cu and $Mo_2C$. Therefore, the use of CO chemisorption will overestimate the site density and underestimate the turnover frequencies over $Cu/Mo_2C$. Nevertheless, as $Mo_2C$ accounts for 94.2 wt % (based on ICP analysis) for this catalyst, CO chemisorption still provides a reasonable estimate of the site density.

**Reaction Rate and Selectivity Measurements.** All of the reactions were performed in a 50 mL Parr Instruments reactor (Micro 5500). The reactor system was equipped with a programmable temperature controller and a magnetic drive for the impeller. The gas phase reactor effluent was analyzed using gas chromatography (Varian 450 with flame ionization and thermal conductivity detectors). Liquid samples (0.4 mL) were periodically withdrawn during the reaction using a dip tube, which was equipped with a 20 $\mu$m filter to separate the liquid from the solid catalyst particles. These liquid samples were analyzed offline using gas chromatography (Varian 450 with flame ionization detector). As gas chromatography showed low responses for formic acid, NMR ($d_6$-DMSO solvent, dimethylformamide internal standard) was used to quantify the formic acid intermediate in selected liquid samples. In addition to the hydrogenation of $CO_2$, we determined the rates and selectivities for hydrogenation of potential intermediates including formic acid and formate ester.

Prior to the reactions, the commercial Cu-based catalysts were reduced in the reactor vessel at 200 °C for 4 h under a flowing mixture of 4% $H_2/N_2$ (50 mL/min). Due to the pyrophoricity of $Mo_2C$ catalysts, the materials were first treated with deaerated water to form a slurry to avoid bulk oxidation of the materials. The slurry was then quickly transferred to the reactor vessel, where it was dried in $H_2$ (50 mL/min) at 110 °C for 2 h. The dried catalyst was then heated to 300 °C at a rate of 4.2 °C/min and reduced at 300 °C under $H_2$ flowing at 100 mL/min for 4 h. The amount of catalyst loaded into the reactors was 200 mg unless otherwise noted.

Solvents for the reactions contained 37.5 mL of 1,4-dioxane (anhydrous, Acro Organics) and 10 $\mu$L of *n*-decane (Acro Organics) as an internal standard. In this study, 1,4-dioxane was selected as the solvent given its solubility for methanol, relatively high boiling point (101 °C), and stability/inertness during the reaction. Other solvents including toluene and tetrahydrofuran (THF) were considered but were not utilized due to their low solubility for methanol (0.1 g methanol/100 g Toluene) and poor separation for GC analysis, respectively. Although ethanol was used as the solvent by Fan et al.,[11] a major limitation was that ethanol altered the reaction pathway, making it difficult to distinguish the methanol produced from $CO_2$ or via formate intermediate. Note that we carried out a series of experiments to investigate the facilitating effect of ethanol on reaction pathways by adding a small amount of ethanol to the 1,4-dioxane solvent as described later.

For the $CO_2$ hydrogenation experiments, the reactors were charged with 10 bar of $CO_2$ and 30 bar of $H_2$ through a dip tube after purging the solvents with $H_2$ for 15 min to remove dissolved oxygen. As we are also interested in combining heterogeneous and homogeneous catalysts to generate a cascade system for $CO_2$ hydrogenation, the reactions were carried out at 135 °C, a temperature at which the homogeneous catalysts reported by Huff et al. are active.[10] Under these conditions, the solubilities for $CO_2$ and $H_2$ are approximately 1.5 and 0.14 mol/L, respectively, based on information in the literature.[30] For selected reactions, 2 mL of ethanol was added to 35.5 mL of 1,4-dioxane. For the formic acid and ethyl formate hydrogenation experiments, 3 mmol of formic acid (98%, Alfa Aesar) or 0.6 mmol of ethyl formate (99.9%, Acro Organics) were added to the solvent, respectively. The reactant mixture was purged with 99.9% $H_2$ (for 15 min) to remove any oxygen and was then charged with 30 bar of $H_2$. The reactor was heated at a rate of 5 °C/min from room temperature to 135 °C and then agitated at a constant rate of 300 rpm, which indicated the start of the reaction. The reactor was maintained at 135 °C through the reaction. Reaction rates for $CO_2$, formic acid, and ethyl formate hydrogenation were calculated on the basis of formation rates for the products (on a $C_1$ basis) or consumption rates for the reactants. Carbon balances closed to within ±8% for all of the experiments. The turnover frequencies (TOF) were determined by normalizing the rates by the surface site densities. The selectivity is defined as the molar ratio of a specific product over the total products.

## RESULTS

**Surface and Physical Properties.** The surface areas, surface site densities, Cu contents, and Cu crystallite sizes for the catalysts are listed in Table 1. The $Mo_2C$ and $Cu/Mo_2C$ catalysts had surface areas in excess of 100 $m^2/g$, the commercial Cu−Zn−Al and Cu−Cr catalysts possessed moderate surface areas, and the nano-Cu material had a relatively low surface area, as expected. The decreased surface area for the $Cu/Mo_2C$ catalyst (135 $m^2/g$) compared to the $Mo_2C$ catalyst (150 $m^2/g$) was likely due to partial blocking of pores in the $Mo_2C$ by Cu nanoparticles. Nevertheless, the

**Table 1. Surface and Physical Properties for the Cu- and $Mo_2C$-Based Catalysts**

| catalyst | surface area ($m^2/g$) | surface site density ($\mu$mol/g) | Cu content (wt %)[a] | average Cu crystallite size (nm) |
|---|---|---|---|---|
| nano-Cu | 5.5 | | 100 | 254 |
| Cu−Zu−Al | 60 | 192[b] | 33 | 89 |
| Cu−Cr | 46 | 184 | 36 | 163 |
| $Mo_2C$ | 151 | 406 | 0 | NA |
| $Cu/Mo_2C$ | 135 | 298 | 5.8 | 34 |

[a]Cu contents for the Cu−Zn−Al, Cu−Cr, and nano-Cu catalysts were obtained from vendor specifications. [b]From ref 29.



DOI: 10.1021/cs501656x
ACS Catal. 2015, 5, 1717−1725

surface area for the Cu/$Mo_2C$ catalyst was comparable to those reported for other $Mo_2C$-supported metals synthesized using similar conditions (e.g., Pt/$Mo_2C$ with 133 $m^2/g$[25b]). The 5.8 wt % Cu loading was equivalent to ~40% of a monolayer on the $Mo_2C$ support assuming atomic dispersion and $10^{19}$ atoms/$m^2$.[27] The surface site densities for all of the materials were in the range of (1.3−2.4) × $10^{18}$ sites/$m^2$ or 13−24% surface coverage assuming $10^{19}$ total sites/$m^2$.

Diffraction patterns for the catalysts are illustrated in Figure 2. The pattern for the Cu−Zn−Al catalyst clearly indicated the presence of Cu and ZnO crystallites, whereas the $Al_2O_3$ phase was amorphous by X-ray diffraction. The XRD pattern for the Cu−Cr catalyst contained peaks for Cu; there was also a peak at 54° 2$\theta$ that is consistent with the presence of CuO within the Cu−Cr ($Cu/Cr_2CuO_4$) catalyst. The pattern for the nano-Cu material showed intense Cu peaks and confirmed its phase purity. As expected, the Cu crystallite sizes for the nano-Cu material were the largest among the other Cu containing catalysts due to the lack of Cu dispersion. The bulk $Mo_2C$ and Cu/$Mo_2C$ materials exhibited peaks for $\beta$-$Mo_2C$ and $\alpha$-$MoC_{1-x}$[29] with similar proportions of each phase based on the relative peak areas. Because the overall Mo to C ratio approaches 2, these materials will be referred to as "$Mo_2C$" in this paper. No peaks were observed for molybdenum oxides ($MoO_2$ or $MoO_3$) in patterns for the carbides, indicating complete carburization during the synthesis. For the Cu/$Mo_2C$ material, there was a broad peak at 41° 2$\theta$ corresponding to the Cu (111) reflection. This result is consistent with a high degree of dispersion for the Cu crystallites on the $Mo_2C$ surface. Table 1 lists crystallite sizes for all of the catalysts.

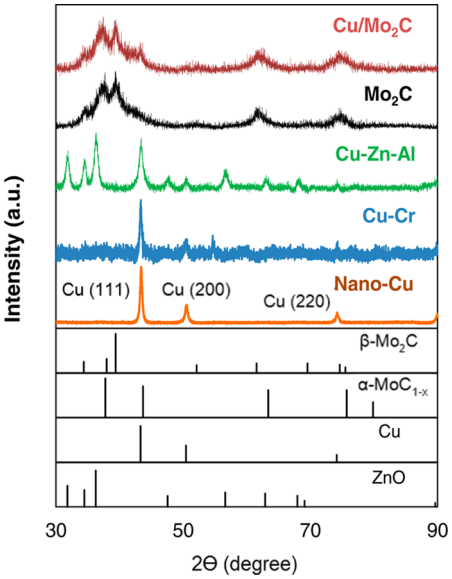


**Figure 2.** X-ray diffraction patterns for the Cu- and $Mo_2C$-based catalysts: $\beta$-$Mo_2C$ (JCPDF 00035-0787), $\alpha$-$MoC_{1-x}$ (JCPDF 00-015-0457), Cu (JCPDF 01-085-1326), and ZnO (JCPDF 01-080-3004).

**Reaction Rates and Selectivities.** *$CO_2$ Hydrogenation.* With the exception of the nano-Cu catalyst, all of the materials were active for the conversion of $CO_2$. The rates and selectivities after 2 h of reaction are listed in Table 2. The Cu−Zn−Al and Cu/$Mo_2C$ catalysts possessed the highest rates, $CH_3OH$ selectivities, and $CH_3OH$ production TOFs. Given the system detection limits (5 ppm), products from the nano-Cu catalyst would have easily been detected if rates per surface area for this material were of the same order as those for the other catalysts. The lack of activity could be a consequence of support effects.[9b,31] There is significant literature suggesting the need for an oxide to function synergistically with Cu.[8a,c,32] The importance of the support is also reflected in the different TOFs for the Cu−Zn−Al, Cu−Cr, and Cu/$Mo_2C$ catalysts. The $Mo_2C$ catalyst was slightly more active than the Cu−Cr catalyst but was much less active and selective than the Cu−Zn−Al and Cu/$Mo_2C$ catalysts, producing significant amounts of CO and some $CH_4$. In comparing the $Mo_2C$ and Cu/$Mo_2C$ catalysts, we observed that the addition of Cu to $Mo_2C$ resulted in a significant increase in activity and a reduction in the CO and $CH_4$ selectivities.

To investigate the potential of formic acid and formate ester intermediates, a series of experiments were carried out in which ethanol (to facilitate esterification of formic acid to ethyl formate), formic acid, or ethyl formate was added to the $CO_2$/$H_2$ reactant. Ethyl formate was used instead of methyl formate to allow easy distinction of $CH_3OH$ produced during $CO_2$ hydrogenation from that produced during formate hydrogenation. The introduction of 50 mmol of ethanol (2 mL) to the $CO_2$ and $H_2$ reactants resulted in the formation of ethyl formate and $CH_3OH$ for all of the catalysts as shown in Table 3. The overall $CO_2$ conversion rates were significantly enhanced after the addition of ethanol. The increase in the $CO_2$ conversion rate was greatest for the Cu−Cr catalyst, which exhibited a very high selectivity and formation rate relative to ethyl formate. This finding suggested that formate hydrogenation to $CH_3OH$ was rate limiting for this catalyst. For the other catalysts, the introduction of ethanol caused a significant increase in the $CH_3OH$ formation rate. The increased $CH_3OH$ formation rates on the addition of ethanol are consistent with formic acid formation being the rate-limiting step. Indeed, as shown in Figure 3, the addition of formic acid (3 mmol) caused a significant increase in the $CH_3OH$ production rate for the Cu/$Mo_2C$ catalyst. Finally, we note that the addition of ethyl formate (2.5 mmol) also caused an increase in the $CH_3OH$ production rate, although the increase was not as substantial as

**Table 2. $CO_2$ Hydrogenation over the Cu- and $Mo_2C$-Based Catalysts[a]**

| | $CO_2$ conv rate | | selectivity (%) | | | | |
|---|---|---|---|---|---|---|---|
| catalyst | $\mu$mol/$g_{cat}$/h | $\mu$mol/$m^2$/h | $CH_3OH$ | $CH_4$ | CO | $CH_3OH$ production rate ($\mu$mol/$m^2$/h) | $CH_3OH$ production TOF ($s^{-1}$ × $10^4$) |
| nano-Cu | 0 | 0 | 0 | 0 | 0 | 0 | 0 |
| Cu−Zn−Al | 168 | 2.8 | 100 | 0 | 0 | 2.8 | 2.4 |
| Cu−Cr | 29 | 0.6 | 88 | 0 | 12 | 0.54 | 0.38 |
| $Mo_2C$ | 83 | 0.5 | 79 | 5.3 | 16 | 0.43 | 0.44 |
| Cu/$Mo_2C$ | 225 | 1.7 | 93 | 2.6 | 4.1 | 1.6 | 2.0 |

[a]135 °C, 10 bar of $CO_2$, 30 bar of $H_2$, 37.5 mL of 1,4-dioxane, rates calculated at 2 h.



DOI: 10.1021/cs501656x
ACS Catal. 2015, 5, 1717−1725

Table 3. $CO_2$ Hydrogenation in the Presence of Ethanol over the Cu- and $Mo_2C$-Based Catalysts[a]

| | $CO_2$ conv rate | | selectivity (%) | | | $HCO_2Et$[b] production | | $CH_3OH$ production | |
|---|---|---|---|---|---|---|---|---|---|
| catalyst | $\mu$mol/$g_{cat}$/h | $\mu$mol/$m^2$/h | $HCO_2Et$[b] | $CH_3OH$ | $CH_4$ + CO | rate ($\mu$mol/$m^2$/h) | TOF ($s^{-1} \times 10^4$) | rate ($\mu$mol/$m^2$/h) | TOF ($s^{-1} \times 10^4$) |
| Cu−Zn−Al | 325 | 5.4 | 36 | 61 | 3.5 | 1.9 | 1.7 | 3.3 | 2.9 |
| Cu−Cr | 269 | 5.8 | 97 | 3.0 | 0 | 5.7 | 3.9 | 0.18 | 0.12 |
| Cu/$Mo_2C$ | 458 | 3.4 | 29 | 66 | 4.8 | 1.0 | 1.2 | 2.2 | 2.8 |

[a]135 °C, 10 bar of $CO_2$, 30 bar of $H_2$, 2 mL of ethanol, 35.5 mL of 1,4-dioxane, rates calculated at 2 h. [b]$HCO_2Et$ = ethyl formate.

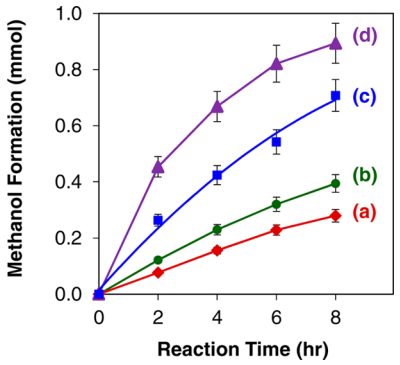


**Figure 3.** Methanol formation during $CO_2$ hydrogenation over the Cu/$Mo_2C$ catalyst with (a) $CO_2$ and $H_2$, (b) $CO_2$ and $H_2$ with 50 mmol of ethanol added, (c) $CO_2$ and $H_2$ with 2.5 mmol of ethyl formate added, and (d) $CO_2$ and $H_2$ with 3 mmol of formic acid added. The experiments were carried out at 135 °C with 10 bar of $CO_2$, 30 bar of $H_2$, and 35.5−37.5 mL of 1,4-dioxane.

when formic acid was added to the $CO_2/H_2$ reactant; ethanol was also observed, confirming ethyl formate hydrogenation.

*Formic Acid Hydrogenation.* All of the catalysts were active for the conversion of formic acid, although $CO_2$ was the principal product. Rates and selectivities after 2 h of reaction are listed in Table 4. The highest surface area specific rate was observed for the nano-Cu catalyst, but the formic acid was almost exclusively converted to $CO_2$. The conversion of formic acid to $CO_2$ ($\Delta G_{135\ °C}$ = −72 kJ/mol) is thermodynamically more favorable than the production of $CH_3OH$ ($\Delta G_{135\ °C}$ = −46.3 kJ/mol) under the reaction conditions that were employed.[33] Activities for the Cu/$Mo_2C$ and Cu−Zn−Al catalysts were similar; the $CH_3OH$ selectivity for the Cu/$Mo_2C$ catalyst was slightly higher than that for the Cu−Zn−Al catalyst. As anticipated, the $Mo_2C$ catalyst was less active and less selective toward $CH_3OH$ production compared to the Cu/$Mo_2C$ catalyst. Both of these catalysts produced methyl formate, $CH_4$, and CO. The enhanced $CH_3OH$ selectivity for the Cu/$Mo_2C$ catalyst compared to the $Mo_2C$ and nano-Cu catalysts suggested a synergy between the $Mo_2C$ and Cu. The Cu−Cr catalyst was the least active and selective for $CH_3OH$ production from formic acid.

*Ethyl Formate Hydrogenation.* With the exception of the nano-Cu catalyst, all of the other catalysts were similarly active. The reaction rates and selectivities after 2 h of reaction are shown in Table 5. Again we used ethyl formate instead of methyl formate to allow easy distinction of the products. It is interesting to note that the Cu−Cr catalyst was nearly as active as the other supported Cu catalysts. Recall that the Cu−Cr catalyst was highly active for ethyl formate formation from $CO_2$ in the presence of ethanol but was relatively inactive for $CH_3OH$ formation from $CO_2$ (with and without ethanol) or formic acid hydrogenation. These results suggested that $CO_2$ inhibited the conversion of ethyl formate to $CH_3OH$ over the Cu−Cr catalyst. This finding will be considered in the selection of catalysts for the cascade system.

Stoichiometrically, the hydrogenation of ethyl formate should produce equal amounts of methanol and ethanol. Methanol to ethanol ratios for the catalysts ranged from 0.4 to 0.7, lower than the stoichiometric value of unity. These results indicated that side reactions occurred. A plausible source for the excess ethanol is the hydrolysis of ethyl formate. This reaction would produce ethanol and formic acid, a likely source of the $CO_2$ produced by most of the catalysts. In fact, the excess ethanol was comparable to the amount of $CO_2$ produced. In addition to $CH_3OH$, ethanol, and $CO_2$, small amounts of $CH_4$ were produced over the $Mo_2C$-containing catalysts. $CH_4$ formation was also observed for these catalysts during $CO_2$ and formic acid hydrogenation.

*Cascade $CO_2$ Hydrogenation.* Our primary objective was to design a cascade system for the hydrogenation of $CO_2$ based on heterogeneous catalysts. To this end, we identified catalysts that would facilitate $CO_2$ hydrogenation to $CH_3OH$ through a formate intermediate. In the presence of ethanol, the Cu−Cr catalyst was highly active and selective for $CO_2$ hydrogenation to ethyl formate. This catalyst was not, however, active for ethyl formate hydrogenation in the presence of ethanol. Several of the catalysts were active for the hydrogenation of ethyl formate in the presence of ethanol; however, we selected the Cu/$Mo_2C$ catalyst due to its high rate and selectivity to $CH_3OH$. Equal masses of the Cu−Cr and Cu/$Mo_2C$ catalysts were used for the cascade system given their similar rates for the hydrogenation

Table 4. Formic Acid Hydrogenation over the Cu and $Mo_2C$-Based Catalysts[a]

| | formic acid conv rate | | selectivity (%) | | | | | $CH_3OH$ production rate | $CH_3OH$ production TOF |
|---|---|---|---|---|---|---|---|---|---|
| catalyst | mmol/$g_{cat}$/h | $\mu$mol/$m^2$/h | $CH_3OH$ | $HCO_2Me$[b] | $CH_4$ | CO | $CO_2$ | ($\mu$mol/$m^2$/h) | ($s^{-1} \times 10^4$) |
| nano-Cu | 1.7 | 300 | 4.6 | 0.0 | 0.0 | 0.0 | 95 | 14 | |
| Cu−Zn−Al | 2.1 | 36 | 27 | 0.0 | 0.0 | 0.0 | 73 | 9.7 | 8.4 |
| Cu−Cr | 3.8 | 84 | 1.8 | 0.0 | 0.0 | 0.3 | 98 | 1.5 | 1.0 |
| $Mo_2C$ | 3.4 | 22 | 15 | 5.2 | 0.8 | 2.7 | 77 | 3.3 | 3.4 |
| Cu/$Mo_2C$ | 3.7 | 28 | 30 | 8.2 | 0.5 | 1.9 | 59 | 8.3 | 11 |

[a]135 °C, 30 bar of $H_2$, 3 mmol of formic acid, 37.5 mL of 1,4-dioxane, rates calculated at 2 h. [b]$HCO_2Me$ = methyl formate.



DOI: 10.1021/cs501656x
ACS Catal. 2015, 5, 1717−1725

**Table 5. Ethyl Formate Hydrogenation over Cu and $Mo_2C$-Based Catalysts[a]**

| | ethyl formate conv rate | | selectivity (%) | | | | | |
|---|---|---|---|---|---|---|---|---|
| catalyst | $\mu$mol/$g_{cat}$/h | $\mu$mol/$m^2$/h | $CH_3OH$ | $C_2H_5OH$ | $CH_4$ | $CO_2$ | $CH_3OH$ production rate ($\mu$mol/$m^2$/h) | $CH_3OH$ production TOF ($s^{-1} \times 10^4$) |
| nano-Cu | 79 | 14 | 37 | 54 | 0 | 9.2 | 10 | |
| Cu−Zn−Al | 598 | 10 | 25 | 55 | 0 | 20 | 4.4 | 3.8 |
| Cu−Cr | 554 | 12 | 27 | 52 | 0 | 21 | 6.0 | 4.1 |
| $Mo_2C$ | 889 | 5.9 | 21 | 53 | 1.9 | 24 | 2.3 | 2.3 |
| Cu/$Mo_2C$ | 837 | 6.2 | 33 | 51 | 0.6 | 16 | 3.7 | 4.6 |

[a]135 °C, 30 bar of $H_2$, 0.6 mmol of ethyl formate, 37.5 mL of 1,4-dioxane, rates calculated at 2 h.

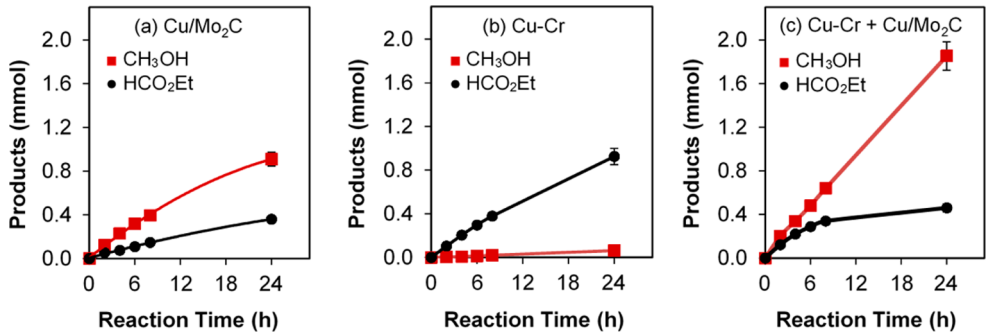


**Figure 4.** Products formation (red squares, methanol; black circles, ethyl formate) during $CO_2$ hydrogenation in the presence of ethanol (2 mL) over the (a) Cu−Cr, (b) Cu/$Mo_2C$, and (c) a mixture of the Cu−Cr and Cu/$Mo_2C$ catalysts. The experiments were carried out at 135 °C with 10 bar of $CO_2$, 30 bar of $H_2$, and 35.5 mL of 1,4-dioxane.

of $CO_2$ to ethyl formate and ethyl formate to $CH_3OH$, respectively.

The $CH_3OH$ and ethyl formate produced as a function of time for the individual Cu−Cr and Cu/$Mo_2C$ catalysts and the mixture of the two in the presence of ethanol are illustrated in Figure 4. Over the Cu/$Mo_2C$ catalyst (Figure 4a), $CH_3OH$ was the major product (~74% selectivity), accompanied by a smaller amount of ethyl formate (~20%). The improved methanol formation rate (after the introduction of ethanol) indicated that ethyl formate was an intermediate. In contrast, for the Cu−Cr catalyst (Figure 4b), ethyl formate was the principal product (~97% selectivity), and its subsequent hydrogenation to methanol was inhibited. For a mixture of the Cu/$Mo_2C$ and Cu−Cr catalysts (Figure 4c), $CH_3OH$ production was enhanced by ~60%, whereas the formation of ethyl formate decreased by a similar amount, compared to the combined amounts for the individual catalysts. These results suggested that the Cu/$Mo_2C$ and Cu−Cr catalysts worked cooperatively to hydrogenate $CO_2$ to $CH_3OH$ via the ethyl formate intermediate. The cascade system achieved a $CO_2$ conversion rate of 416 $\mu$mol/$g_{cat}$/h and $CH_3OH$ and ethyl formate selectivities of 77 and 20%, respectively, after 24 h of reaction. The corresponding $CH_3OH$ TOF (calculated at 2 h) for the system is $4.7 \times 10^{-4}$ $s^{-1}$.

Given the $CH_3OH$ formation rates for some of the catalysts, we also considered a cascade system to convert $CO_2$ to dimethyl ether via $CH_3OH$ intermediate. The Cu−Zn−Al and Cu/$Mo_2C$ catalysts were most active for the hydrogenation of $CO_2$ to $CH_3OH$. Zeolitic catalysts such as HZSM-5 are known to dehydrate $CH_3OH$ to dimethyl ether and at high temperatures to hydrocarbons via the methanol to olefins (MTO) process or methanol to gasoline (MTG).[3b,5] Figure 5 illustrates the methanol and dimethyl ether formed as a function of time for the individual Cu/$Mo_2C$ and HZSM-5 catalysts as well as the mixture. The results suggested that the

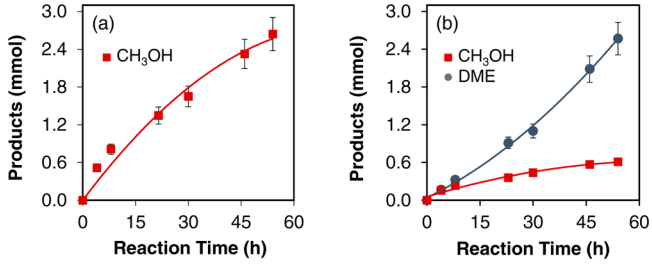


**Figure 5.** Methanol and dimethyl ether (DME) production from $CO_2$ hydrogenation over (a) Cu/$Mo_2C$ catalyst (600 mg) and (b) a mixture of Cu/$Mo_2C$ and HZSM-5 catalysts (600 mg each). The experiments were carried out at 135 °C with 10 bar of $CO_2$, 30 bar of $H_2$, 37.5 mL of 1,4-dioxane, for 54 h. The HZSM-5 catalyst alone was not active under these conditions.

Cu/$Mo_2C$ and HZSM-5 catalysts worked in concert to produce dimethyl ether from $CO_2$ via methanol intermediate.

## DISCUSSION

Results for the Cu−Zn−Al and Cu−Cr catalysts are somewhat different from those reported by Fan et al.[11] They did not observe $CH_3OH$ production at temperatures below ~150 °C; the only products were ethyl formate and CO. The methanol selectivity was maximum (~60%) at 200 °C. We observed relatively high selectivities (>75%) for all of the catalysts at 135 °C (Table 2). There are several plausible explanations for differences between our results and those reported by Fan et al.[11] Their experiments were carried out with ethanol as the solvent; we used 1,4-dioxane. Although $H_2$ solubilities for these solvents are similar (0.16 and 0.14 mol/L for ethanol[34] and 1,4-dioxane,[30a] respectively), the $CO_2$ solubilities are very different (0.14 and 1.5 mol/L, respectively[30b,35]). In addition, their use of ethanol would facilitate the esterification reaction and could accelerate methanol production. Finally, it is possible that the


DOI: 10.1021/cs501656x
ACS Catal. 2015, 5, 1717−1725

catalysts were in different states of reduction. Our protocol included a step to pretreat the catalysts prior to measurement of their rates and selectivities. The protocol described by Fan et al.[11] did not include a pretreatment step. It has been reported that $Cu^0$ is the active species for methanol synthesis;[8b,9b] therefore, one would expect lower activities for the untreated oxide catalysts.

Turnover frequency is a measure of the intrinsic activity of a catalyst. There are no reported TOFs that can be compared directly with our results; however, at 220−240 °C and 10−80 bar, TOFs for $CH_3OH$ production have been reported in the range of 0.003−0.018 $s^{-1}$ for Cu-based catalysts.[36] Extrapolating these published rates to 135 °C would yield TOFs on the order of $10^{-4}$ $s^{-1}$ using the reported activation energy of ∼60 kJ/mol.[8a] The estimated TOF for the Cu−Cr:Cu/$Mo_2C$ cascade system was $4.7 \times 10^{-4}$ $s^{-1}$. Huff and Sanford reported a $CH_3OH$ production turnover number of 2.5 at 135 °C after 16 h for a homogeneous cascade system incorporating $(PMe_3)_4$Ru-(Cl)(OAc), Sc$(OTf)_3$, and (PNN)Ru(CO)(H) complexes. The corresponding TOF would be $4.3 \times 10^{-5}$ $s^{-1}$.[10] Interestingly, they reported a methanol turnover number that would be equivalent to a TOF of $3.6 \times 10^{-4}$ $s^{-1}$ for a cascade system where $CO_2$ hydrogenation to formic acid and formic acid esterification were carried out at 75 °C and then the formate was hydrogenated at 135 °C in a separate reactor (without the first two catalysts). This TOF is similar in magnitude to that achieved for the heterogeneous catalysts described in this paper.

By comparing the $CH_3OH$ production rates from the hydrogenation of $CO_2$ and suspected intermediates (formic acid and ethyl formate), we were able to further investigate the reaction pathways reported by Fan et al.[11] and propose rate-limiting steps. Figure 6 illustrates reaction pathways that are

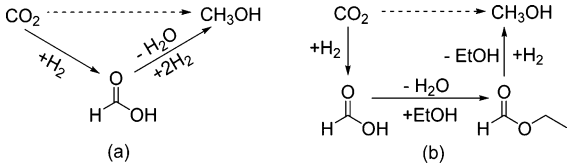


**Figure 6.** Summary of reaction pathways for $CO_2$ hydrogenation over the Cu- and $Mo_2C$-based catalysts (a) in the absence of ethanol and (b) in the presence of ethanol.

most consistent with our results. In the absence of ethanol, formic acid is likely the principal intermediate. In the presence of ethanol, the pathway from $CO_2$ to $CH_3OH$ seemed to include formic acid and formate intermediates. Our results are consistent with the hydrogenation of $CO_2$ to formic acid being the rate-limiting step for most of the Cu- and $Mo_2C$-based catalysts. We also observed a small amount of CO production, perhaps via the reverse water−gas shift over most of the catalysts (Tables 2 and 3). To investigate the possibility that CO was an intermediate during $CO_2$ hydrogenation to methanol, we performed CO hydrogenation at the same reaction conditions (135 °C, 10 bar of CO, 30 bar of $H_2$). Over the Cu/$Mo_2C$ catalyst, the $CH_3OH$ TOF from CO hydrogenation was $4.9 \times 10^{-6}$ $s^{-1}$, equivalent to ∼2.5% of the $CH_3OH$ TOF ($2.0 \times 10^{-4}$ $s^{-1}$) during $CO_2$ hydrogenation. Similarly, over the Cu−Zn−Al catalyst, the $CH_3OH$ produced from CO hydrogenation was only ∼0.8% of that from $CO_2$ hydrogenation. These results suggested that the CO hydrogenation did not contribute significantly to the production of $CH_3OH$ under the $CO_2$ hydrogenation conditions employed.

Results for the $Mo_2C$ and Cu/$Mo_2C$ catalysts suggested a synergy between Cu and $Mo_2C$. We expect that the Cu was zerovalent based on prior investigations.[27] Vidal et al. reported evidence of synergy between Cu or Au and TiC (support) during gas phase $CO_2$ hydrogenation to methanol.[37] These metals are effective sites for hydrogen dissociation. Synergistic effects between the metal and carbide have also been reported for Pt/$Mo_2C$ catalysts during water−gas shift[25b] and Pd/WC catalysts during the selective hydrogenation of triglycerides.[38] It is plausible that Cu particles on the Cu/$Mo_2C$ catalyst enhanced the hydrogen surface coverage, thereby facilitating the hydrogenation of $CO_2$. We also note that the synergy has been reported between Cu and oxides, such as ZnO, in the associated catalysts.[8a,c,32] To investigate the long-term stability of $Mo_2C$-based materials, $CO_2$ hydrogenation was performed over the Cu/$Mo_2C$ catalyst for 72 h. The $CH_3OH$ TOF initially decreased from $2.0 \times 10^{-4}$ $s^{-1}$ (at 4 h) to $0.6 \times 10^{-4}$ $s^{-1}$ (at 22 h) and then remained relatively constant. The spent catalyst was characterized using XRD and showed the same phases as the fresh catalyst.

To the best of our knowledge, the cascade system described in this paper (Figure 7) is the first of its kind for $CO_2$

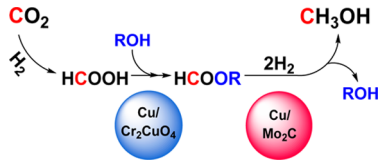


**Figure 7.** Schematic of proposed reaction pathway for the Cu−Cr and Cu/$Mo_2C$ catalytic cascade system.

hydrogenation. Clearly better-performing catalysts would lead to superior overall performance. Of particular interest would be catalysts for the hydrogenation of $CO_2$ to formic acid or formate. Xu et al. recently reported that a silica-supported Ir catalyst (Ir-PN/SBA-15) was highly active for the conversion of $CO_2$ to formic acid at 120 °C with 20 bar of $CO_2$ and 20 bar of $H_2$ in an aqueous solution containing small amounts of triethylamine.[39] One could also consider combining homogeneous catalysts with heterogeneous catalysts. The homogeneous catalysts described by Huff and Sanford[10] would be good candidates, although compatibility of the homogeneous and heterogeneous catalysts would have to be assessed.

## CONCLUSIONS

In this paper we describe a novel heterogeneous cascade system for the hydrogenation of $CO_2$ to methanol through a formate intermediate. This system consisted of Cu−Cr and Cu/$Mo_2C$ catalysts and yielded a turnover frequency of $4.7 \times 10^{-4}$ $s^{-1}$ for $CH_3OH$ production at 135 °C. The results encourage the development of other cascade systems of this type. We also observed that a Cu/$Mo_2C$ catalyst was active for $CO_2$ hydrogenation to methanol. The deposition of Cu onto the $Mo_2C$ surface enhanced the methanol formation rates. These $Mo_2C$-based materials were also active for formic acid and formate ester hydrogenation. The introduction of ethanol during $CO_2$ hydrogenation resulted in improved methanol production rates over the Cu/$Mo_2C$ and Cu−Zn−Al catalysts. We attribute this to the accelerated formation of ethyl formate and its subsequent hydrogenation to methanol. In contrast, the


DOI: 10.1021/cs501656x
ACS Catal. 2015, 5, 1717−1725

Cu−Cr catalyst was selective for the production of ethyl formate; its subsequent conversion to methanol was inhibited by $CO_2$. The production of dimethyl ether from $CO_2$ was also demonstrated over a Cu/$Mo_2C$:HZSM-5 cascade system, where $CO_2$ was hydrogenated to methanol over Cu/$Mo_2C$ and methanol was further converted to dimethyl ether by HZSM-5.

## AUTHOR INFORMATION


### Corresponding Author

*E-mail: ltt@umich.edu (L.T.T.).


### Notes

The authors declare no competing financial interest.

## ACKNOWLEDGMENTS

We acknowledge funding from the National Science Foundation, under the CCI Center for Enabling New Technologies through Catalysis (CENTC) Phase II Renewal (CHE-1205189). We thank Dr. Jason Gaudet, Dr. Tanya Breault, and Brian Wyvratt for assistance with the experiments and data analysis. We also thank Dr. Chelsea Huff, Dr. Tim Brewster, Prof. Alex Miller, Prof. Karen Goldberg, and Prof. Melanie Sanford for helpful discussions.

## REFERENCES


(1) *International Energy Outlook 2014*; U.S. Energy Information Administration, U.S. Department of Energy, Office of Integrated and International Energy Analysis: Washington, DC, USA, 2014.

(2) Metz, B.; Davidson, O. R.; Bosch, P. R.; Dave, R.; Meyer, L. A. *Climate Change 2007: Mitigation*; Contribution of Working Group III to the Fourth Assessment Report of the Intergovernmental Panel on Climate Change: Cambridge, UK, 2007.

(3) (a) Quadrelli, E. A.; Centi, G.; Duplan, J.; Perathoner, S. *ChemSusChem* **2011**, *4*, 1194−1215. (b) Centi, G.; Iaquaniello, G.; Perathoner, S. *ChemSusChem* **2011**, *4*, 1265−1273. (c) Centi, G.; Quadrelli, E. A.; Perathoner, S. *Energy Environ. Sci.* **2013**, *6*, 1711−1731.

(4) Howarth, R. W.; Bringezu, S. *Biofuels: Environmental Consequences and Interactions with Changing Land Use*; Proceedings of the Scientific Committee on Problems of the Environment (SCOPE) International Biofuels Project Rapid Assessment, Gummersbach, Germany, Sept 2008.

(5) Keil, F. J. *Microporous Mesoporous Mater.* **1999**, *29*, 49−66.

(6) Fukuda, H.; Kondo, A.; Noda, H. *J. Biosci. Bioeng.* **2001**, *92*, 405−416.

(7) (a) Olah, G. A.; Goeppert, A.; Prakash, G. K. S. *J. Org. Chem.* **2008**, *74*, 487−498. (b) Olah, G. A.; Prakash, G. K. S.; Goeppert, A. *J. Am. Chem. Soc.* **2011**, *133*, 12881−12898.

(8) (a) Choi, Y.; Futagami, K.; Fujitani, T.; Nakamura, J. *Appl. Catal., A* **2001**, *208*, 163−167. (b) Natesakhawat, S.; Lekse, J. W.; Baltrus, J. P.; Ohodnicki, P. R.; Howard, B. H.; Deng, X.; Matranga, C. *ACS Catal.* **2012**, *2*, 1667−1676. (c) Kurtz, M.; Bauer, N.; Büscher, C.; Wilmer, H.; Hinrichsen, O.; Becker, R.; Rabe, S.; Merz, K.; Driess, M.; Fischer, R. A. *Catal. Lett.* **2004**, *92*, 49−52. (d) Wang, W.; Wang, S.; Ma, X.; Gong, J. *Chem. Soc. Rev.* **2011**, *40*, 3703−3727.

(9) (a) Yang, Y.; Evans, J.; Rodriguez, J. A.; White, M. G.; Liu, P. *Phys. Chem. Chem. Phys.* **2010**, *12*, 9909−9917. (b) Behrens, M.; Studt, F.; Kasatkin, I.; Kühl, S.; Hävecker, M.; Abild-Pedersen, F.; Zander, S.; Girgsdies, F.; Kurr, P.; Kniep, B.-L.; Tovar, M.; Fischer, R. W.; Nørskov, J. K.; Schlögl, R. *Science* **2012**, *336*, 893−897.

(10) Huff, C. A.; Sanford, M. S. *J. Am. Chem. Soc.* **2011**, *133*, 18122−18125.

(11) Fan, L.; Sakaiya, Y.; Fujimoto, K. *Appl. Catal., A* **1999**, *180*, L11−L13.

(12) Yu, K. K. M.; Tsang, S. C. *Catal. Lett.* **2011**, *141*, 259−265.

(13) (a) Inoue, T.; Fujishima, A.; Konishi, S.; Honda, K. *Nature* **1979**, *277*, 637−638. (b) Kuwabata, S.; Nishida, K.; Tsuda, R.; Inoue, H.; Yoneyama, H. *J. Electrochem. Soc.* **1994**, *141*, 1498−1503. (c) Barton, E. E.; Rampulla, D. M.; Bocarsly, A. B. *J. Am. Chem. Soc.* **2008**, *130*, 6342−6344. (d) Hori, Y. Electrochemical $CO_2$ reduction on metal electrodes. In *Modern Aspects of Electrochemistry*; Springer: Berlin, Germany, 2008; pp 89−189. (e) Centi, G.; Perathoner, S. *Catal. Today* **2010**, *150*, 151−162.

(14) Kumar, B.; Llorente, M.; Froehlich, J.; Dang, T.; Sathrum, A.; Kubiak, C. P. *Annu. Rev. Phys. Chem.* **2012**, *63*, 541−569.

(15) (a) Canfield, D.; Frese, K., Jr. *J. Electrochem. Soc.* **1983**, *130*, 1772−1773. (b) Tomkiewicz, M.; Woodall, J. M. *Science* **1977**, *196*, 990−991.

(16) Wesselbaum, S.; vom Stein, T.; Klankermayer, J.; Leitner, W. *Angew. Chem., Int. Ed.* **2012**, *124*, 7617−7620.

(17) Wasilke, J.-C.; Obrey, S. J.; Baker, R. T.; Bazan, G. C. *Chem. Rev.* **2005**, *105*, 1001−1020.

(18) (a) Felpin, F.-X.; Fouquet, E. *ChemSusChem* **2008**, *1*, 718−724. (b) Yamada, Y.; Tsung, C.-K.; Huang, W.; Huo, Z.; Habas, S. E.; Soejima, T.; Aliaga, C. E.; Somorjai, G. A.; Yang, P. *Nat. Chem.* **2011**, *3*, 372−376.

(19) Huff, C. A.; Kampf, J. W.; Sanford, M. S. *Organometallics* **2012**, *31*, 4643−4645.

(20) Davies, I. W.; Matty, L.; Hughes, D. L.; Reider, P. J. *J. Am. Chem. Soc.* **2001**, *123*, 10139−10140.

(21) Yang, C.; Ma, Z.; Zhao, N.; Wei, W.; Hu, T.; Sun, Y. *Catal. Today* **2006**, *115*, 222−227.

(22) Dubois, J.-L.; Sayama, K.; Arakawa, H. *Chem. Lett.* **1992**, *21*, 5−8.

(23) Xu, W.; Ramirez, P.; Stacchiola, D.; Rodriguez, J. *Catal. Lett.* **2014**, *144*, 1−7.

(24) (a) Vo, D.-V. N.; Adesina, A. A. *Appl. Catal., A* **2011**, *399*, 221−232. (b) Xiang, M.; Li, D.; Xiao, H.; Zhang, J.; Qi, H.; Li, W.; Zhong, B.; Sun, Y. *Fuel* **2008**, *87*, 599−603. (c) Patterson, P. M.; Das, T. K.; Davis, B. H. *Appl. Catal., A* **2003**, *251*, 449−455.

(25) (a) Patt, J.; Moon, D.; Phillips, C.; Thompson, L. *Catal. Lett.* **2000**, *65*, 193−195. (b) Schweitzer, N. M.; Schaidle, J. A.; Ezekoye, O. K.; Pan, X.; Linic, S.; Thompson, L. T. *J. Am. Chem. Soc.* **2011**, *133*, 2378−2381.

(26) Ren, H.; Yu, W.; Salciccioli, M.; Chen, Y.; Huang, Y.; Xiong, K.; Vlachos, D. G.; Chen, J. G. *ChemSusChem* **2013**, *6*, 798−801.

(27) Schaidle, J. A.; Schweitzer, N. M.; Ajenifujah, O. T.; Thompson, L. T. *J. Catal.* **2012**, *289*, 210−217.

(28) Klug, H. P.; Alexander, L. E. *X-Ray Diffraction Procedures: For Polycrystalline and Amorphous Materials*, 2nd ed.; Wiley-VCH: Weinheim, Germany, 1974; Vol. 1, p 992.

(29) Schaidle, J. A.; Lausche, A. C.; Thompson, L. T. *J. Catal.* **2010**, *272*, 235−245.

(30) (a) Brunner, E. *J. Chem. Eng. Data* **1985**, *30*, 269−273. (b) Kassim, D.; Zainel, H.; Al-Asaf, S.; Talib, E. *Fluid Phase Equilib.* **1988**, *41*, 287−294.

(31) (a) Günter, M. M.; Ressler, T.; Jentoft, R. E.; Bems, B. *J. Catal.* **2001**, *203*, 133−149. (b) Kasatkin, I.; Kurr, P.; Kniep, B.; Trunschke, A.; Schlögl, R. *Angew. Chem.* **2007**, *119*, 7465−7468.

(32) Fujitani, T.; Nakamura, J. *Appl. Catal., A* **2000**, *191*, 111−129.

(33) Thermodynamic calculations are based on standard values from NIST Chemistry WebBook.

(34) Purwanto; Deshpande, R.; Chaudhari, R.; Delmas, H. *J. Chem. Eng. Data* **1996**, *41*, 1414−1417.

(35) Dalmolin, I.; Skovroinski, E.; Biasi, A.; Corazza, M.; Dariva, C.; Oliveira, J. V. *Fluid Phase Equilib.* **2006**, *245*, 193−200.

(36) (a) Słoczyński, J.; Grabowski, R.; Kozłowska, A.; Olszewski, P.; Stoch, J.; Skrzypek, J.; Lachowska, M. *Appl. Catal., A* **2004**, *278*, 11−23. (b) Arena, F.; Barbera, K.; Italiano, G.; Bonura, G.; Spadaro, L.; Frusteri, F. *J. Catal.* **2007**, *249*, 185−194. (c) Sun, Q.; Zhang, Y.-L.; Chen, H.-Y.; Deng, J.-F.; Wu, D.; Chen, S.-Y. *J. Catal.* **1997**, *167*, 92−105.




DOI: 10.1021/cs501656x
*ACS Catal.* 2015, 5, 1717−1725

(37) Vidal, A. B.; Feria, L.; Evans, J.; Takahashi, Y.; Liu, P.; Nakamura, K.; Illas, F.; Rodriguez, J. A. *J. Phys. Chem. Lett.* **2012**, *3*, 2275−2280.
(38) Lausche, A. C.; Okada, K.; Thompson, L. T. *Electrochem. Commun.* **2012**, *15*, 46−49.
(39) Xu, Z.; McNamara, N. D.; Neumann, G. T.; Schneider, W. F.; Hicks, J. C. *ChemCatChem* **2013**, *5*, 1769−1771.



DOI: 10.1021/cs501656x
*ACS Catal.* 2015, 5, 1717−1725